OXFORD

Human Molecular Genetics, 2015, Vol. 24, No. 25 7221–7226

doi: 10.1093/hmg/ddv422
Advance Access Publication Date: 28 October 2015
Original Article

ORIGINAL ARTICLE

Reduced PLP2 expression increases ER-stress-induced neuronal apoptosis and risk for adverse neurological outcomes after hypoxia ischemia injury

Lilei Zhang[1,2], Tao Wang[1] and David Valle[1,*]

[1]Institute of Genetic Medicine, School of Medicine, Johns Hopkins University, Baltimore, MD, USA and [2]Department of Genetics and Genome Sciences, School of Medicine, Case Western Reserve University, Cleveland, OH, USA

*To whom correspondence should be addressed at: Johns Hopkins University, Broadway Research Building, 519, 733 Broadway, Baltimore, MD 21287, USA. Tel: +1 410 955 2460; Fax: +1 410 955 7397; Email: dvalle@jhmi.edu

Abstract

Both genetic and environmental factors contribute to the development of intellectual disability (ID). Previously, we identified a promoter variant (–113C>A) in *PLP2* (proteolipid protein 2) that results in an ∼4-fold reduction of transcript and protein and is overly represented in males with X-linked ID (XLID). The functional connection between reduced PLP2 expression and increased risk to XLID is unknown. To investigate the pathophysiological mechanisms, we studied a *Plp2*-loss-of-function murine model and fibroblasts from XLID patients hemizygous for *PLP2*-(–113C>A). We found that *Plp2*-deficient mouse embryonic fibroblast and human fibroblasts carrying *PLP2*-(–113C>A) have similarly defective endoplasmic reticulum (ER) trafficking, increased basal ER stress and exaggerated susceptibility to inducers of ER stress. *Plp2*-deficient mice show increased neuronal death to ER stress and hypoxia *in vitro* and in a neonatal hypoxia-ischemia model *in vivo*. Finally, we provide evidence that up-regulation of PLP2 directly promotes resistance to ER stressors. Results of our studies support the hypothesis that reduced PLP2 expression increase susceptibility of neurons to environmental ER stressors such as hypoxia and ischemia and that increased apoptosis and neuronal death contribute to the risks to ID in humans.

Introduction

Neonatal hypoxia-ischemia encephalopathy (HIE) contributes to injuries to the developing brain and frequently results in variable degrees of developmental delay, cerebral palsy, behavioral anomalies and intellectual disability (ID) (1,2). It has long been hypothesized that genetic susceptibility interacting with recognizable environmental factors contribute to increased risks, severity and neurological outcome of infants with HIE. Despite extensive investigations, conclusive genetic evidence supporting this hypothesis remains elusive (3).

Proteolipid protein 2 (PLP2) is a small integral membrane protein of the endoplasmic reticulum (ER). PLP2 expresses abundantly in multiple brain regions including hippocampus but its function is not known. In a previous cDNA microarray-based genetic screen to identify novel genes responsible for XLID, we found a *PLP2* promoter variant (–113C>A) that is over-represented in a cohort of males with XLID (4). Further molecular studies indicate that *PLP2*-(–113C>A) alters the core-binding site of ETS family transcription factors and decreases the expression of PLP2 by 3- to 4-fold both *in vitro* and *in vivo* (4). However, the function of PLP2 and how it relates to the pathophysiology of ID are unknown.

To investigate the mechanisms in detail, we produced and characterized *Plp2*-deficient mice and studied human fibroblasts carrying *PLP2*-(–113C>A). Here, we provide *in vitro* and *in vivo* evidence that PLP2 deficiency leads to increased sensitivity to ER-stress agents and hypoxic-ischemic injury in both murine

Received: May 18, 2015. **Revised:** September 26, 2015. **Accepted:** October 5, 2015

model and human cells. Our results support that reduced level of PLP2 leads to increased genetic susceptibility to ER stressors such as HIE and contributes to increased risks of early brain injuries and development of ID later in life.

Results

To study the molecular function of *Plp2*, we generated knockout mice by inserting a LacZ-neo cassette into the exon 1 of *Plp2*, six codons downstream of the initiation methionine (Supplementary Material, Fig. S1). We did not detect *Plp2* transcript or protein in *Plp2*-deficient mice by northern blot or western blot, respectively, in samples from multiple tissues (Supplementary Material, Fig. S2A and B). *Plp2*-deficient mice were born in Mendelian ratio and show normal litter size, physical growth, general appearance, ambulatory activities and mating behaviors when compared with their wild-type littermates. As expected, female mice show random X-inactivation in multiple tissues (Supplementary Material, Fig. S3C).

Next, we derived primary mouse embryonic fibroblasts (MEFs) from the $Plp2^{-/Y}$ mice (KO) and their $Plp2^{+/Y}$ littermates (WT) to examine the cellular consequences of *Plp2* deficiency. We noted that the peripheral ER in the KO cells seems dilated comparing to the fine network observed in the WT cells (Fig. 1A). Exposure to thapsigargin (Thap), a selective inhibitor of the Ca^{2+}-ATPase of the ER caused the ER of the KO cells to fragment and disperse, whereas the WT cells showed dilated but not fragmented ER (Fig. 1B). This effect was specific for the ER, as there was no difference in other organelles, such as the lysosomes shown here, labeled with a LAMP-1 antibody. To confirm these observations, we performed electron microscopy on WT and KO MEFs. These ultra-structural studies showed that the ER lumen is markedly dilated in the KO cells under basal conditions (Fig. 1C, upper images). Cells of both genotypes showed dilated and fragmented ER to a similar extent after exposure to Thap (Fig. 1C, bottom images).

We suspected that these changes in ER morphology might reflect abnormal ER trafficking. To test this hypothesis, we used a temperature sensitive GFP tagged vesicular stomatitis virus G (ts-VSVG) protein that exits the ER at 32°C, but not at 40°C (5). We visualized trafficking of ts-VSVG in cells labeled with fluorescent ER and Golgi makers. In WT MEFs, 15 min after shifting to the permissive temperature (32°C), most of the ts-VSVG remained in the ER but by 45 min, a substantial amount has reached the Golgi with all cells show some ts-VSVG in the Golgi. By 90 min, the ts-VSVG has reached its final destination, the plasma membrane. In contrast, in KO cells, most of the ts-VSVG remains in the ER and fails to reach the Golgi even at 90 min (Fig. 1D–F). ER to Golgi movement of ts-VSVG is associated with sialylation of the recombinant protein with a concomitant decrease in mobility on SDS–PAGE. After 45 min at 32°C, the lysate from WT cells showed additional band with reduced mobility consistent with sialylated ts-VSVG reaching the mid-Golgi. In contrast, in the KO cells, essentially all ts-VSVG showed faster mobility suggesting ER localization (Fig. 1F). Taken together,

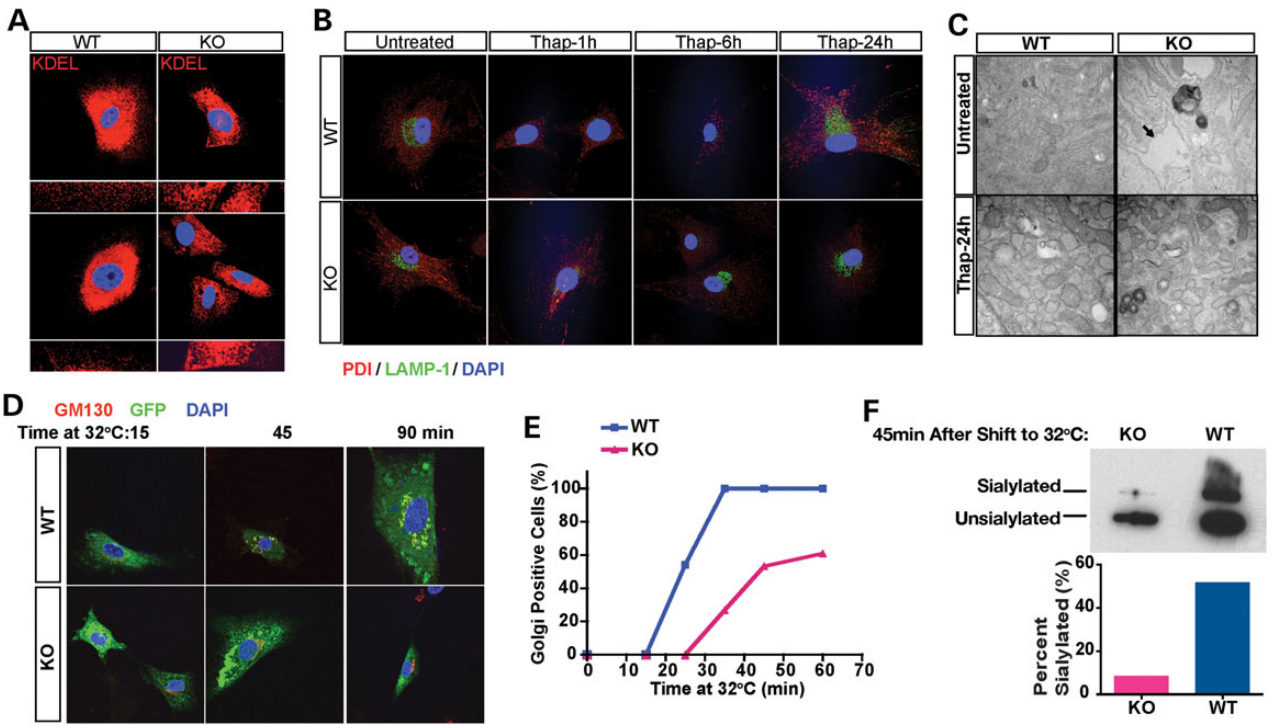

Figure 1. *Plp2*-deficient MEFs show dilated ER and defective ER-Golgi trafficking. (**A**) WT and KO MEFs were examined by confocal microscopy (400×) after staining with antibody specific for KDEL (red). Two representative fields of each genotype are shown with the peripheral ER of cells in each field shown at higher magnification (1000×) below. Nuclei were stained with DAPI (blue). (**B**) WT and KO MEFs were treated with Thap for the indicated times. ER and lysosome morphology were labeled with antibody specific for PDI (red) and LAMP-1 (green), respectively. Nuclei were stained with DAPI (blue). (**C**) Transmission electron microscopy of WT and KO MEFs with and without Thap treatment. Arrow points to the markedly dilated ER in the untreated KO MEFs. (**D–F**) Trafficking assay of WT and KO MEFs. (D) Immunofluorescence with antibody specific for the Golgi marker, GM130 (red). Nuclei were stained with DAPI (blue); ts-VSVG-GFP is shown in green. Note the co-localization of ts-VSVG-GFP with GM130 shown in yellow in the merged images. (E) Cells were counted under confocal microscopy. For each time point at least 100 cells were scored by an observer blinded to genotype, and the percentage of cells that show GFP positive in the Golgi is plotted on the y-axis. (F) Western blot. ts-VSVG was detected with antibody specific for GFP, and the unsialylated and sialylated forms reflect the ER form and Golgi-modified form of ts-VSVG-GFP, respectively.

these observations show that deficiency of *Plp2* is associated with ER dilatation and delayed trafficking of ER proteins.

Abnormal trafficking of ER proteins may activate ER stress and, if not resolved, lead to cell death by apoptosis (6). As we did not observe significant cell death at baseline, we challenged WT or KO MEFs with various types of cell death stimuli. MEFs of both genotypes showed comparable sensitivity to VP16 (etoposide, an intrinsic pathway stimulus) and FasL (anti-Fas antibody plus cycloheximide, an extrinsic pathway stimulus) (Fig. 2A). In contrast, Thap leads to significantly increased cell death in KO MEFs compared with WT MEFs. Similarly, sensitivity to a different ER stressor, tunicamycin (TUN), an inhibitor of N-linked glycosylation, was also increased in the KO MEFs (Fig. 2A). Further, after treatment with Thap or TUN, KO MEFs displayed increased apoptotic markers, including cleaved caspase 3, and PARP, as well as specific ER stress markers, cleaved caspase12 and GRP78. Conversely, cells of both genotypes had a similar response to FasL (Fig. 2B). Additionally, we noted increased basal level of ER stress in the KO MEFs, as evident by the increased cleavage of caspase 12 and slight induction of GRP78, which is consistent with our immunofluorescence and electron microscopy observations of abnormal ER morphology under basal conditions (Fig. 1A–C). Thus, we show *Plp2*-deficiency results in impaired ER trafficking and increased sensitivity to ER-stress-induced cell death, but does not affect sensitivity to agents that stimulate the mitochondria or Fas ligand-induced apoptotic pathways.

Previously, we identified a common human promoter variant that decreases the expression of PLP2 in fibroblasts and lymphoblasts by 4-fold (4). We next explored whether the reduced PLP2 expression in these individuals is sufficient to convey an increase in the susceptibility to ER-stress-induced apoptosis. We exposed passage number matched primary human fibroblasts of known PLP2 genotype to Thap or TUN and found that after treatment fibroblasts from two males hemizygous for the *PLP2-(−113C>A)* variant showed large vacuoles that filled the cytoplasm, whereas fibroblasts from males hemizygous for the wild-type allele showed only minimal changes under the identical condition (Fig. 2C). Consistent with the result of the KO MEF cells, fibroblasts hemizygous for the *PLP2-(−113C>A)* variant also exhibited 3-fold higher cell death when exposed to Thap and no difference in response to Fas ligand. Unlike the MEFs, however, these human fibrobalsts with decreased PLP2 showed a small difference in sensitivity to VP16 (Fig. 2D). Our results indicate that despite the residue PLP2 expression, human fibroblasts hemizygous for the PLP2 promoter variant phenocopy the KO mice at least at

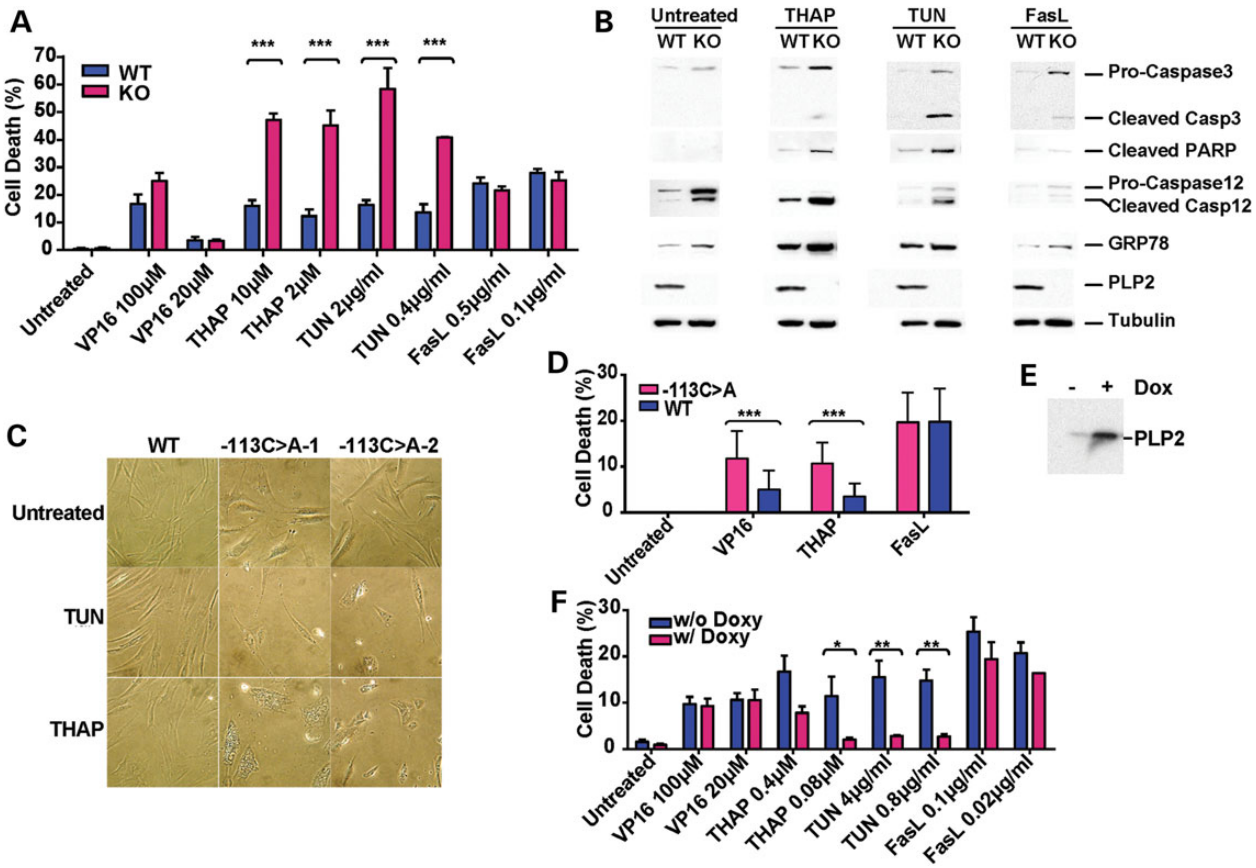

Figure 2. *Plp2* deficiency leads to increased susceptibility to ER stress. (**A**) WT and KO MEFs cell death assay. Data are shown as mean ± SEM; $n = 6$; ***$P < 0.001$. (**B**) WT and KO MEFs at passage 5 were treated with Fas ligand (2 μg/ml), Thap (10 mm) or TUN (2 μM) for 24 h. Total cells (adherent and floating) were harvested for western blot. (**C**) Human primary fibroblasts from two males who carry the PLP2-(−113C>A) allele and one normal control (WT) were exposed to TUN (20 μg/ml) and Thap (10 μM) for 48 h. 200× light microscopy. (**D**) Human primary fibroblasts from two males who carry *PLP2-(−113C>A)* allele and three normal males (WT) were treated with VP-16 (200 μM), Thap (10 μM) and Fas ligand (0.1 μg) + cycloheximide (20 μg/ml) for 48 h. The range was indicated with the error bar (***$P < 0.001$). (**E**) Flp-In Trex 293-PLP2 cells were cultured in medium with or without doxycyclin (1 μg/ml) for 24 h. Western blotted with an antibody specific for PLP2. (**F**) Flp-In Trex 293-PLP2 cells cultured in medium with (blue, PLP2 over-expressing) or without doxycycline (red, non-PLP2 over-expressing) were incubated in media containing various apoptotic inducing agents at the indicated doses for 24 h. Data are shown as mean ± SEM; $n = 3$; *$P < 0.05$; **$P < 0.01$.

the cellular level, thus providing support for investigating the human pathophysiology using the KO mouse model at hand.

We then sought to test if increased levels of PLP2 may protect cells from ER-stress agents. We used HEK 293 cells for their low level of endogenous PLP2 and a sensitive apoptotic response to ER-stress-inducing agents. We established a stable HEK 293 cell line that expresses PLP2 from a single locus under the control of doxycycline induction (Flp-In T-REx HEK293-PLP2). In the presence of doxycycline, PLP2 is induced to ~10-fold higher than baseline at the protein level (Fig. 2E). As expected, this high level of PLP2 expression did not affect sensitivity to VP16 or FasL, but dramatically decreased cell death in response to both Thap and TUN (Fig. 2F). This result strongly supports our hypothesis that levels of PLP2 influence the cellular response to ER stress. It further suggests that therapeutic intervention to enhance PLP2 expression at critical developmental stages may be beneficial for humans carrying the *PLP2-(−113C>A)* promoter variant.

Bear in mind the human ID phenotype we have associated with the common promoter variant of *PLP2*, we extended our study to 7-day primary cultures of cortical neurons isolated from the WT and KO embryos, and exposed the cells to either TUN or STS (staurosporine, a broad-spectrum kinase inhibitor, intrinsic pathway). Consistent with the MEF studies, *Plp2*-deficient neurons (KO) displayed increased sensitivity to TUN, but not to STS (Fig. 3A). ER stress is an integral component of hypoxia-ischemia neuronal injury (7). We next attempted to simulate conditions that mimic ischemia-reperfusion injury in culture; primary cortical neurons were transiently exposed to medium containing 20 mM 2-deoxy-glucose and 5 mM KCN for 1 h, then allowed to recover in standard medium for 24 h (8). *Plp2*-deficient neurons displayed a significant increase in cell death induced by these culture conditions compared with WT neurons (Fig. 3A).

Hypoxic-ischemic injury during neonatal period is a common cause to developmental delays and ID in humans. Because HIE is a known ER stressor (7), we thus explored if reduced PLP2 expression contributes to increased risks and severity of neuronal death and brain damage caused by HIE. To study potential effects of HIE *in vivo*, we used an adaptation of the Vannucci neonatal hypoxic-ischemic model for rodents (9,10). We subjected WT and KO littermates ($n = 12$) at postnatal day 7 (P7) to permanent unilateral common carotid artery (CCA) ligation, followed by hypoxia for 90 min in 8% oxygen. We sacrificed the mice and harvested their brains for analysis 5 days after the insult (Fig. 3B–F). We measured the hippocampal area in eight consecutive serial sections 400 µm apart through the caudal diencephalons and calculated the ratio of ipsi-lateral versus contra-lateral hippocampal area. At all levels, this ratio in the KO is smaller than that of the WT suggesting more pronounced tissue loss (Fig. 3C). We also derived the volume ratios of the ipsi-lateral versus contra-lateral hippocampi from the area ratio and distance between consecutive sections. The volume ratio of the KO was 0.45, indicating the injury reduces hippocampal volume by about half, whereas the volume ratio in the WT littermates was 0.95, indicating the injury barely reduces hippocampal volume (Fig. 3D). Thus, the volume of injury following hypoxic-ischemic injury in the KO animals (55%, 1–45%) is ~10 times higher than that of the WT littermates (5%, 1–95%). Consistent with this finding, we observed

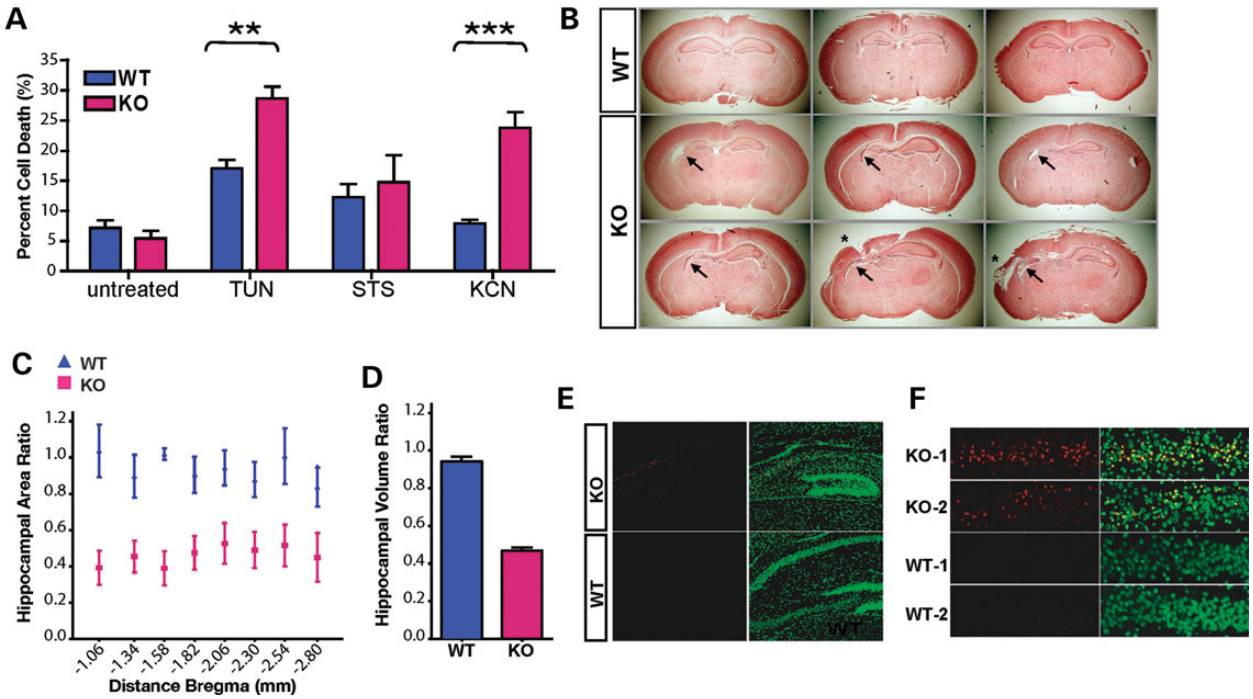

Figure 3. Plp2 deficiency leads to increased neuronal death in response to ER stress and hypoxia. (**A**) WT and KO primary cortical neurons were treated with TUN (10 µg/ml) or STS (0.02 µM) for 48 h, or KCN (5 µM/2-deoxy-glucose) for 1 h followed by recovery in regular medium for 24 h. Data are shown as mean ± SEM, $n = 6$, $^{**}P < 0.01$; $^{***}P < 0.001$. (**B–F**) Neonatal hypoxic-ischemic brain injury model. (B) Coronal sections were stained with trichrome. Representative images are shown here, each picture is from an individual mouse. The left side of the image corresponds to the right side of the brain ipsi-lateral to the ligated CCA. (C) The hippocampal area was measured at eight consecutive levels at 400 µm distance and expressed as the area of the ipsi-lateral hippocampus/contra-lateral hippocampus. The x-axis is the distance from bregma (mm) according to a standard mouse brain atlas. Data are shown as mean ± SEM, $n = 12$ in each group. (D) Relative volumes of ipsi-/contra-lateral hippocampal area are calculated from the relative area and the distance between each measured areas. Data are shown as mean ± SEM, $n = 12$ in each group, $P = 0.0002$. (E) Sections, containing maximum hippocampus area, were stained with TUNEL staining (red). Nuclei were counter stained with Sytox green. Representative images of the hippocampi ipsi-lateral to the CCA ligation are shown here. (F) Enlarged TUNEL staining of the ipsi-lateral CA1 region of two mice from each genotype.

markedly increased apoptosis in the ipsi-lateral hippocampi of the KO mice when compared with their wild-type littermate controls by TUNEL staining (Fig. 3E and F). We conclude that *Plp2*-deficiency results in greatly increased sensitivity to hypoxic brain injury *in vivo*.

Discussion

In these studies, we show that PLP2 regulates the cellular response to stimuli that converge on the ER-stress pathway. *Plp2* deficiency leads to abnormal ER trafficking, which perturbs ER homeostasis, and renders the ER more susceptible to further environmental stress. We provide evidence that *Plp2* deficiency confers increased susceptibility to apoptosis elicited by known ER stressors in mice both *in vitro* and *in vivo*. We further demonstrate that human fibroblasts carrying a common PLP2 promoter variant causing reduced PLP2 expression have similar cellular phenotype to what we observed in *Plp2*-deficient embryonic fibroblasts and neurons in mice. Importantly, our data show that overexpression of PLP2 protects the cells from ER-stress-induced apoptosis, suggesting PLP2 actively alleviates the cellular stress.

In our previous study, we found that *PLP2*-(−113C>A) is significantly enriched in a large cohort of males with XLID (5.85%) when compared with matched normal control males (1.56%) (4). The minor allele frequency (MAF) observed in our control population is corroborated by data from the 1000 genome project, which showed an MAF (rs.41298450) of 1% overall, 2% in CEU and not found in African descent in Southwest USA. These findings indicate that *PLP2*-(−113C>A) is present at a lower frequency in males with apparent normal cognitive function and is unlikely to be a Mendelian cause for ID.

Our current studies provide strong evidence that *PLP2*-(−113C>A)-mediated reduced expression conveys an increased susceptibility to ER stress. Among the common environmental ER stressors, perinatal HIEs frequently result in severe neurodevelopmental defects including ID. Our studies using a Vannucci neonatal hypoxic-ischemic model support that *Plp2* deficiency in mice is a risk factor to neuronal apoptosis after HIE.

Together, genetic and functional data from our studies suggest that *PLP2*-(−113C>A) conveys an increased risk to ID through a mechanism of increased neuronal death in crucial brain regions post environmental ER stressors such as HIE. Therapeutic manipulation through this transcription factor binding site (−113C>A) could potentially enhance the expression of PLP2 and protect the neurons from ER-stress-induced apoptosis, and thus, may improve the neurological outcome of some of these susceptible individuals following an episode of HIE. Further investigations in these areas are clearly warranted.

Materials and Methods

Additional information can be found in the Supplementary Materials.

ER trafficking assay

WT and KO MEFs were transiently transfected with pEGFP-N1-ts-VSVG by electroporation, plated onto coverslips and allowed to recover at 37°C for 5 h. Cells were then incubated at the non-permissive temperature (40°C) for 12 h, before switching to the permissive temperature (32°C) for the indicated times. Cells were harvest at the indicated times for immunofluorescence staining or western blot.

Cells death assay

Apoptosis is scored by nuclear morphology. The cell count results are data from three independent experiments each with duplicated samples. In each experiment, slides were blinded for genotype and treatment, and at least 400 cells were counted from each slide for each data point.

Neonatal hypoxic-ischemic brain injury model

P7 mice was subjected to right CCA ligation followed by 8% O_2 for 90 min. The brains were harvested 5 days later, fixed in formalin and embedded in paraffin. We made serial 5 µm coronal sections throughout the caudal diencephalons region at 400 µm intervals and stained the sections with trichrome. Images were processed using ImageJ (http://rsb.info.nih.gov/ij/). The hippocampal areas were measured and ipsi-/contra-lateral ratios were calculated at eight coronal levels, and the ratio of volume was calculated.

Statistics

Data are shown in mean ± SEM, Student's *t*-test was used to compare two groups; except for human fibroblast cell death assay, as $n = 2$ for the −113C>A genotype, data are presented as mean ± range for this experiment (Fig. 2D). A *P*-value of <0.05 is considered significant.

Supplementary Material

Supplementary Material is available at *HMG* online.

Conflict of Interest statement. None declared.

Funding

This work was supported by an Institutional award from the Johns Hopkins University Brain Science initiative and National Institute of Mental Health (P50MH094268) to D.V. and RO1HD052680 to T.W.

References

1. Sran, S.K. and Baumann, R.J. (1988) Outcome of neonatal strokes. *Am. J. Dis. Child.*, **142**, 1086–1088.
2. Sreenan, C., Bhargava, R. and Robertson, C.M. (2000) Cerebral infarction in the term newborn: clinical presentation and long-term outcome. *J. Pediatr.*, **137**, 351–355.
3. Sheldon, R.A., Sedik, C. and Ferriero, D.M. (1998) Strain-related brain injury in neonatal mice subjected to hypoxia-ischemia. *Brain Res.*, **810**, 114–122.
4. Zhang, L., Jie, C., Obie, C., Abidi, F., Schwartz, C.E., Stevenson, R.E., Valle, D. and Wang, T. (2007) X chromosome cDNA microarray screening identifies a functional PLP2 promoter polymorphism enriched in patients with X-linked mental retardation. *Genome Res.*, **17**, 641–648.
5. Presley, J.F., Cole, N.B., Schroer, T.A., Hirschberg, K., Zaal, K.J. and Lippincott-Schwartz, J. (1997) ER-to-Golgi transport visualized in living cells. *Nature*, **389**, 81–85.
6. Breckenridge, D.G., Germain, M., Mathai, J.P., Nguyen, M. and Shore, G.C. (2003) Regulation of apoptosis by endoplasmic reticulum pathways. *Oncogene*, **22**, 8608–8618.
7. Paschen, W., Althausen, S. and Doutheil, J. (1999) Ischemia-induced changes in 2′-5′-oligoadenylate synthethase mRNA levels in rat brain: comparison with changes produced by

perturbations of endoplasmic reticulum calcium homeostasis in neuronal cell cultures. *Neurosci. Lett.*, **263**, 109–112.
8. Chae, S.S., Paik, J.H., Allende, M.L., Proia, R.L. and Hla, T. (2004) Regulation of limb development by the sphingosine 1-phosphate receptor S1p1/EDG-1 occurs via the hypoxia/VEGF axis. *Dev. Biol.*, **268**, 441–447.
9. Vannucci, R.C., Brucklacher, R.M. and Vannucci, S.J. (1996) The effect of hyperglycemia on cerebral metabolism during hypoxia-ischemia in the immature rat. *J. Cereb. Blood Flow Metab.*, **16**, 1026–1033.
10. Vannucci, R.C. and Vannucci, S.J. (1997) A model of perinatal hypoxic-ischemic brain damage. *Ann. NY Acad. Sci.*, **835**, 234–249.